Plasma-Deposited Polymeric Films Prepared from Carbonyl-Containing Volatile Precursors: XPS Chemical Derivatization and Static SIMS Surface Characterization

Ashutosh Chilkoti, Buddy D. Ratner,* and David Briggs†

Department of Chemical Engineering and Center for Bioengineering, BF-10, University of Washington, Seattle, Washington 98195

Received March 22, 1990

The surface chemistry of plasma-deposited films (PDF) created from carbonyl precursors was investigated by Fourier transform infrared spectroscopy (FTIR), X-ray photoelectron spectroscopy (XPS), and vapor-phase derivatization reactions in conjunction with XPS (derivatization XPS). The selectivity of trifluoroacetic anhydride (TFAA) toward hydroxyl groups and hydrazine toward carbonyl groups was ascertained by reacting them with various polymers with oxygen-containing functional groups likely to be present in the carbon–oxygen PDF of interest. Investigation of the surface chemistry of ultrathin PDF from acetaldehyde, acetone, and 2-butanone demonstrated that under the invariant experimental conditions utilized, the effect of varying the C/O ratio of the precursor had little effect on PDF surface chemistry. The low concentration of carbonyl groups detected suggests extensive fragmentation of the precursor during plasma deposition. The creation of a graded series of oxygen-containing PDF was also explored by blending controlled ratios of O_2 gas in the acetone feed to the plasma reactor. Derivatization XPS indicated that the distribution of hydroxyl, carbonyl, and carboxyl functional groups varied across the range of oxygen incorporation in the acetone–O_2 PDF. The surface chemistry of the acetone–O_2 PDF series and a commercial tissue culture polystyrene surface (Falcon) was compared by XPS, derivatization XPS, and static secondary ion mass spectrometry.

Introduction

Plasma-deposited films (PDF) have been used to alter the surface properties of substrates for a wide variety of applications. However, our knowledge regarding the surface chemistry of these films is fragmentary and incomplete. In part, this is related to the lack of suitable surface analytical techniques capable of probing the structure of these ultrathin films (with thicknesses frequently on the order of 10–1000 Å). The problem is exacerbated by the complex nature of PDF, which are frequently multifunctional and display varying degrees of unsaturation and cross-linking.[1,2]

In view of the above, elucidation of the surface structure of such thin films calls for the application of a multitechnique approach. XPS coupled with chemical derivatization methods was used as the primary analytical technique in this investigation. While the direct application of XPS is capable of providing the atomic composition in the surface region of PDF, it is of limited utility in identifying the oxygen-containing functional groups present on their surfaces. This is due to the multiplicity of oxygen-containing species present, many of which have virtually indistinguishable binding energy (BE) shifts.[3] Information about the type and concentration of functional groups on the surfaces of plasma treatments and PDF is of interest, because it may help clarify the role these species play in mediating diverse phenomena, ranging from cell spreading and growth on surfaces[4-6] to interfacial adhesion.[7-9]

The use of derivatization techniques in conjunction with XPS (derivatization XPS) allows for the semiquantitative estimation of functional groups of interest.[10-12] This approach has great utility for the analysis of polymer surfaces that are not amenable to interrogation by direct XPS analysis.[3] However, the artifact-free use of derivatization XPS for the analysis of complex polymers such as PDF requires characterization of the reaction in terms of selectivity of the reagent toward the functional group of interest, its XPS detectibility, an approximate knowledge of the kinetics of the reaction, and the stability of the derivatized species under analysis conditions.[11,12] With these concerns in mind, the reactions used in this study have been so characterized.

Static secondary ion mass spectrometry (SIMS) has been shown to provide valuable insights into the surface structure of conventional and surface-modified polymers.[13-22] Preliminary data on the use of static SIMS to

* Author to whom correspondence should be addressed.
† ICI PLC, Wilton Materials Research Centre, P.O. Box 90, Wilton, Middlesbrough, Cleveland TS6 8JE, U.K.

(1) Morosoff, N.; Patel, D. L. *A.C.S. Polym. Prepr.* **1986**, *27*, 82.
(2) Ohno, M.; Ohno, K.; Sohma, J. *J. Polym. Sci.* **1987**, *25*, 1273.
(3) Dilks, A. In *Electron Spectroscopy: Theory, Techniques, and Applications*; Baker, A. D., Brundle, C. R., Eds.; Academic: London, 1981; Vol IV, p 277.
(4) Ramsey, W. S.; Hertl, W.; Nowlan, E. D.; Binkowski, W. J. *In Vitro* **1984**, *20*, 802.
(5) Curtis, A. S. G.; Forrester, J. V.; McInnes, C.; Lawrie, F. *J. Cell Biol.* **1983**, *97*, 1500.
(6) Curtis, A. S. G.; Forrester, J. V.; Clark, P. *J. Cell Sci.* **1986**, *86*, 9.
(7) Briggs, D.; Kendall, C. R. *Int. J. Adhes. Adhes.* **1982**, *2*, 13.
(8) Briggs, D. *J. Adhes.* **1982**, *13*, 287.
(9) Briggs, D.; Kendall, C. R. *Polymer* **1979**, *20*, 1053.
(10) Batich, C. D. *Appl. Surf. Sci.* **1988**, *32*, 57.
(11) Batich, C. D.; Wendt, C. R. In *A.C.S. Symposium Series*; Dwight, D. W.; Fabish, T. J., Thomas, H. R., Eds.; American Chemical Society: Washington DC, 1981; Vol. 162, p 221.
(12) Everhart, D. E.; Reilley, C. N. *Anal. Chem.* **1981**, *53*, 665.
(13) Gardella Jr., J. A.; Hercules, D. M. *Anal. Chem.* **1980**, *52*, 226.
(14) Gardella Jr., Novak, F. P.; Hercules, D. M. *Anal. Chem.* **1984**, *56*, 1371.
(15) Hearn, M. J.; Ratner, B. D.; Briggs, D. *Macromolecules* **1988**, *21*, 2950.
(16) Hearn, M. J.; Briggs, D.; Yoon, S. C.; Ratner, B. D. *Surf. Interface Anal.* **1987**, *10*, 384.
(17) Lub, J.; van Vroonhoven, F. C. B. M.; Bruninx, E.; Benninghoven, A. *Polymer* **1989**, *30*, 40.
(18) Lub, J.; van Velzen, P. N. T.; van Leyen, D.; Hagenhoff, B.; Benninghoven, A. *Surf. Interface Anal.* **1988**, *12*, 53.
(19) Niehuis, E.; van Velzen, P. N. T.; Lub. J.; Heller, T.; Benninghoven, A. *Surf. Interface Anal.* **1989**, *14*, 135.
(20) Occhiello, E.; Garbassi, F.; Morra, M. *Surf. Sci*, **1989**, *211/212*, 218.
(21) Fakes, D. W.; Davies, M. C.; Brown, A.; Newton, J. M. *Surf. Interface Anal.* **1988**, *13*, 233.

0897-4756/91/2803-0051$02.50/0

Table I. Details of Centrifugal Casting of Model Polymers Used To Study the Selectivity of Derivatization Reactions

polymer	structure	casting soln
poly(*cis*-1,3-butadiene) (PBu)	$[CH_2CH{=}CHCH_2]_n$	2% w/v in chloroform
poly(*cis*-isoprene) (PiP)	$[CH_2CH{=}C(CH_3)CH_2]_n$	2% w/v in chloroform
poly(vinyl alcohol) (PVA)	$[CH_2CH(OH)]_n$	2% w/v in doubly distilled, deionized water
poly(*p*-hydroxystyrene) (PHS)	$[CH_2CH(C_6H_4OH)]_n$	4% w/v in 1,4-dioxane
poly(ethylene oxide) (PEO)	$[CH_2CH_2O]_n$	2% w/v in chloroform
poly(vinyl isobutyl ether) (PVIE)	$[CH_2CH(OCH_2CH(CH_3)_2)]_n$	2% w/v in chloroform
poly(vinyl methyl ketone) (PVMK)	$[CH_2CH(COCH_3)]_n$	1% w/v in chloroform
poly(acrylic acid) (PAA)	$[CH_2CH(CO_2H)]_n$	2% w/v in methanol
poly(ethyl methacrylate) (PEMA)	$[CH_2C(CH_3)(CO_2C_2H_5)]_n$	2% w/v in toluene
poly(vinyl acetate) (PVAc)	$[CH_2CH(O_2CCH_3)]_n$	2% w/v in toluene
polycaprolactone (PCL)	$[O(CH_2)_5CO]_n$	2% w/v in chloroform

compare the surface chemistry of carbon–oxygen PDF created from acetone–O_2 mixtures and a commercial tissue culture polystyrene (TCPS) surface (Falcon) are reported in this paper.

Our interest in PDF stems from their potential to enhance cell growth on substrates such as polystyrene (PS) that by themselves do not support the growth of anchorage-dependent cell lines. It has been demonstrated that plasma-modified surfaces prepared from different plasma polymerizable precursors or etchants display significant differences in their ability to stimulate cell spreading and growth.[23,24] Specifically, carbon–oxygen PDF such as those prepared from acetone and methanol show a pronounced ability to selectively adsorb fibronectin from serum and aggressively promote cell growth.[23] However, differences in precursor chemical structure, precursor nature (plasma depositing versus etching), and the different reaction conditions used for the end modification make it difficult to isolate the underlying factors in the modification process that are responsible for the range of biological responses elicited by these surfaces.

One of the aims of this study was to systematically investigate the role played by the precursor in the surface chemistry of carbon–oxygen PDF of interest. Hence, PDF were prepared from a homologous class of carbonyl-functionalized precursors (i.e., acetaldehyde, acetone, and 2-butanone). This allowed us to study the effect of varying the carbonyl concentration of the precursor upon PDF surface chemistry. Further impetus for pursuing this line of investigation was provided by our desire to optimize these surfaces with respect to cell growth. One part of this optimization has dealt with the reaction conditions, which have been shown to influence PDF chemistry.[25,26] However, optimization of PDF chemistry with respect to the precursor has received little study. Since the surface oxygen concentration of carbon–oxygen PDF can be directly correlated to cell growth,[23,24] optimization of PDF chemistry is of particular relevance to the anticipated end use of these PDF as cell growth substrates.

We also wished to explore other strategies to create carbon–oxygen PDF in a systematic and reproducible fashion that would not only exhibit good cell growth but also be stable in air and in water. One approach to creating oxygen-functionalized polymer surfaces is by corona discharge treatment (CDT)[27,28] or O_2 plasma treatment.[29,30] However, upon exposure to an aqueous medium, these plasma-treated surfaces lose a significant fraction of surface oxygen species.[27,28] Another limitation of using plasma-etching processes to modify the surface of a polymeric substrate is that the ensuing surface functionalization is dependent upon the chemistry of the substrate.[30,31] Thus, plasma-etching processes cannot be applied to widely different substrates in order to achieve similar modifications. Since the PDF created from carbonyl-functionalized precursors were found to be stable both in air and in water, it was thought that using a mixture of plasma polymerizable precursor (e.g., acetone) and oxygen would be a viable method to create stable and oxygen-rich PDF. The former component in the feed would provide a stable organic layer that is lightly functionalized with oxygenated groups, while the latter component would further enrich the oxygen content of these films.

The ultimate aim of preparing such oxygen-rich PDF is to evaluate their cell growth characteristics. In typical cell growth experiments, commercially available TCPS surfaces are frequently used as a control. While the treatment used to modify the PS substrate for commercial tissue cultureware is proprietary, it results in the incorporation of oxygen species on the surface.[31] In prospective applications where not only the oxygen content but the type and concentration of functional groups present may be relevant,[4-6,23,24] a more detailed investigation of the surface chemistry of such a surface modification merits consideration. Information gleaned about the surface chemistry of commercial TCPS surfaces, when compared to other plasma modifications that also incorporate oxygenated species such as the acetone–O_2 PDF, should yield new insights into the surface chemical factors that influence cell growth.

Experimental Section

Materials. Untreated PS substrates were supplied by Corning Glass Works (Horseheads, NY) and were cleaned by ultrasonication in reagent grade ethanol. Poly(ethylene terephthalate) (PET) was acquired as film from Miles Scientific (Naperville, IL) and was cleaned by ultrasonication in toluene, followed by ethanol. Falcon TCPS Petri dishes were acquired from Becton-Dickinson and Co. (Oxnard, CA) and were analyzed as received. Infrared grade KBr powder was purchased from Aldrich Chemicals (Milwaukee, WI). Acetaldehyde, acetone, and 2-butanone were also purchased from Aldrich Chemicals (99% purity). Medical grade O_2 gas was supplied by Air Products and Chemicals Inc. (Allentown, PA). Trifluoroacetic anhydride (TFAA), 2,2,2-trifluoroethanol (TFE), and di-*tert*-butylcarbodiimide (Di-tBuC) were purchased from Aldrich Chemicals (all reagents 99% purity),

(22) Ratner, B. D.; Briggs, D.; Hearn, M.; Yoon, S. C.; Edelman, P. G. In *Surface Characterization of Biomaterials*; Ratner, B. D., Ed.; Elsevier: Amsterdam, 1988; p 317.
(23) Chinn, J. A.; Horbett, T. A.; Ratner, B. D.; Schway, M. B.; Haque, Y.; Hauschka, S. D. *J. Colloid Interface Sci.* **1989**, *127*, 67.
(24) Ertel, S. I.; Horbett, T. A.; Ratner, B. D. *J. Biomed. Mater. Res.*, in press.
(25) Clark, D. T. *Pure Appl. Chem.* **1984**, *54*, 415.
(26) Gombotz, W. R.; Hoffman, A. S. *J. Appl. Polym. Sci., Appl. Polym. Symp.* **1988**, *42*, 255.
(27) Gerenser, L. J.; Elman, J. F.; Mason, M. G.; Pochan, J. M. *Polymer* **1985**, *26*, 1162.
(28) Pochan, J. M.; Gerenser, L. J.; Elman, J. F. *Polymer* **1986**, *27*, 1058.
(29) Clark, D. T.; Wilson, R. *J. Polym. Sci., Polym. Chem. Ed.* **1983**, *21*, 837.
(30) Grant, J. L.; Dunn, D. S.; McClure, D. J. *J. Vac. Sci. Technol. A.* **1989**, *6*, 2213.
(31) Ratner, B. D.; Chilkoti, A.; Lopez, G. P. In *Plasma Deposition of Polymer Films*; D' Agostino, R., Ed.; Academic Press: New York, 1990.

Table II. Plasma Reactor Conditions for the Acetone–O_2 PDF[a]

feed, cm^3 min^{-1}		
acetone	O_2	press, mTorr
1.0[b]	0	51
0.9[b]	0.1	52
0.8	0.2	50
0.7[b]	0.3	55
0.6	0.4	58
0.5[b]	0.5	60
0.4	0.6	63

[a] Power (W) = 5 W, time (t) = 10 min, s = 3.0 × 10^{-6} s^{-1}. [b] Samples prepared at these experimental conditions for set I. Set II samples were prepared at all of the above conditions.

while hydrazine was purchased from Eastman Kodak Co. (Rochester, NY) and from Aldrich Chemicals (99% purity). Pyridine (99% purity) was purchased from EM Science (Cherry Hill, NJ). The model polymers used to test for the specificity of the derivatization reactions were acquired either from Scientific Polymers Inc. (Ontario, NY) or from Polysciences Inc. (Warrington, PA). The polymers were centrifugally cast from appropriate solvents at 4000 rpm, for 20–40 s, using an EC-101 spin coater (Headway Research Inc., Garland, TX). Details of the casting solutions are contained in Table I. The glass disks on which the polymers were centrifugally cast were cleaned by ultrasonication in an Isopanasol (C.R. Callen Co., Seattle, WA) solution (1.5% v/v) and repeated rinses in deionized/reverse osmosis purified water.

Plasma Deposition. The PS samples were placed vertically in the plasma reactor while the KBr powder was spread evenly on a clean glass plate that was then placed horizontally in the reactor. A radio frequency (rf, 13.56 MHz), capacitively coupled plasma reactor (described in ref 23) was used to create the plasma. The precursors, previously subjected to a freeze–thaw cycle under vacuum to remove dissolved air, were introduced into the reactor through a flow controller (UV2-11, Vacuum General, Inc., San Diego, CA). Prior to depositing the plasma films, the substrates were cleaned by an Ar etch at the following conditions: pressure (P) = 175 mTorr, rf power (W) = 30 W, flow rate (F) = 4.0 cm^3 min^{-1}, time (t) = 5 min. To compare the PDF created from the three carbonyl-functionalized precursors, the reaction conditions were kept invariant for all three depositions and were P = 150 mTorr, W = 10 W, F = 4.0 cm^3 min^{-1} (space velocity (v) = 1.2 × 10^{-5} s^{-1}), t = 30 min, unless otherwise noted. After the rf power was switched off, the samples were quenched at the same pressure and flow rate by flowing the precursor through the reactor for 5 min. The selection of experimental parameters for the plasma deposition of the carbonyl precursors was governed by a desire to maintain low power per molecule ratios, under conditions where a stable plasma could be generated for all three precursors. Beyond a deposition time of 2 min we find no dependence of surface chemistry on reaction time, probably because the film thickness is greater than the sampling depth of XPS.

Two sets of acetone–O_2 PDF were prepared at different times. Set II PDF were prepared at seven different flow rates, while set I was comprised of PDF prepared at four of the above flow rates. The reaction conditions used to create the acetone–O_2 PDF are summarized in Table II. These values were selected on the basis of previous experiments that indicated a strong inverse dependence of surface oxygen incorporation on rf power. For the deposition of the acetone–O_2 PDF, the throttle valve (Model MDV-015, Vacuum General, Inc.) used to control the pressure in a feedback loop was disconnected. Thus, the pressures reported in Table II are the final pressures read from the capacitance manometer (CML-11, Vacuum General, Inc.) that were attained after the rf generator (HF-650, ENI Power Systems, Inc., Rochester, NY) had been switched on. The acetone–O_2 PDF were also quenched for 5 min at the same flow rates used for the deposition. Moreover, the reactor was brought up to a pressure of ~8–10 Torr by opening the acetone and oxygen flow controllers (UV2-21, FV6-11, Vacuum General, Inc.) to their maximum values (i.e., 10.0 cm^3 min^{-1}) while isolating the reactor vessel from the mechanical pump. At this time, a valve was opened to bring the reactor pressure to atmospheric. The higher pressure quenching step was instituted in view of the possible greater reactivity of these films toward air. Base pressures in the reactor were typically in the range 2–5 mTorr.

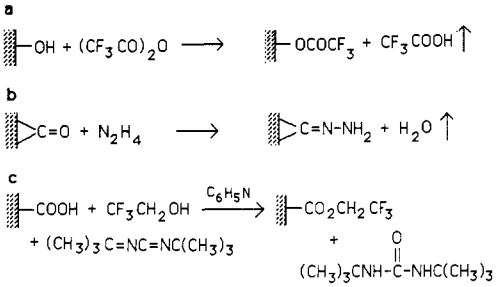

Figure 1. Derivatization reactions: (a) TFAA with OH groups, (b) hydrazine with C=O groups, (c) TFE with COOH groups.

FTIR Analysis. The plasma-deposited KBr powder was pressed into a pellet in a K-13 KBr die, (Beckman Instruments) by using a Carver Laboratory press. FTIR analysis was then carried out in the transmission mode on an Analect FX-6200 instrument. The background signal was acquired on a KBr pellet pressed from untreated powder from the same lot.

Hydroxyl Derivatization Procedure. Samples were derivatized with TFAA vapor, at ambient pressure, to label the hydroxyl group with fluorine. The reaction of a hydroxylated surface with TFAA is shown in Figure 1a. The samples were placed on a glass slide, which was introduced into a glass test tube. TFAA (2 mL) was injected into the test tube, below the glass slide, without contacting the samples. The test tube was then sealed with a Teflon-lined cap, and the reaction with the TFAA vapor was allowed to proceed for 15 min at ~35 °C. The reaction conditions selected were based upon earlier reports in the literature[26-28] and were meant to ensure complete reaction of PDF hydroxyl groups with TFAA vapor. The samples were then recovered and immediately introduced into the SSX-100 surface analysis system (Surface Science Instruments, Mountain View, CA). Poly(vinyl alcohol) (PVA) and untreated PS were derivatized with TFAA as controls.

Carbonyl Derivatization Procedure. PDF and model polymers of interest were derivatized with hydrazine vapor to label the carbonyl group with nitrogen. The reaction of hydrazine with a carbonyl-functionalized surface is shown in Figure 1b. The procedure used for the TFAA derivatization reaction was adopted for the hydrazine derivatization. Derivatizations performed in the first half of this study (i.e., on the acetaldehyde, acetone, and 2-butanone PDF) were carried out for 15 min. Subsequently, experiments on the kinetics of this reaction, using poly(vinyl methyl ketone) (PVMK) as a model compound, indicated that the level of N incorporation attains a steady-state value after ~45 min. Thus, the acetone–O_2 PDF were derivatized for 1 h. PS and PVMK were derivatized with hydrazine along with the samples of interest as controls; the former to verify that adsorbed hydrazine was not retained under ultrahigh vacuum, and the latter to verify the extent of carbonyl derivatization.

Carboxyl Derivatization Procedure. The protocol developed by Lyons et al. for the vapor-phase derivatization for carboxyl groups with TFE/Di-tBuC was used with minor modifications.[32] The reaction of a carboxylated surface with TFE is shown in Figure 1c. The samples were placed on a glass slide and introduced into a glass test tube. TFE (0.9 mL), pyridine (0.4 mL), and Di-tBuC (0.3 mL) were sequentially injected into the test tube (below the glass slide) at 15-min intervals. The test tube was then sealed with a Teflon-lined cap, and the reaction was allowed to proceed at ambient temperature for ~12 h. Poly(acrylic acid) (PAA) and PS control specimens were derivatized along with the samples of interest.

XPS. The XPS experiments were done on a SSX-100 surface analysis system using a monochromatic Al Kα X-ray source, a detection system with a 30° solid angle acceptance, a hemispherical analyzer, and a position sensitive detector. Typical pressures in the analysis chamber during these experiments were ~10^{-9} Torr. All the polymers were analyzed at 55° takeoff angle. The takeoff

(32) Lyons, C. S.; Korba, G. A., personal communication.

angle was defined as the angle between the surface normal and the axis of the analyzer lens. Survey scans (0–1000 eV) were run at 150-eV analyzer pass energy and 1000-μm X-ray spot size to determine the elemental composition of each polymer. The experimental peak areas were numerically integrated and normalized to account for the number of scans, the number of channels per electron volt, the Scofield photoionization cross section,[33] and the sampling depth. The SSX-100 transmission function for a pass energy of 150 eV was assumed to be constant over the appropriate range of photoelectron kinetic energies.[34] The sampling depth was assumed to vary as $KE^{0.7}$, where KE is the kinetic energy of the photoelectrons.[34] Variable takeoff angle XPS experiments were performed using a 6° slit geometry for more accurate depth resolution.[35] Charge compensation was achieved by means of a low-energy flood gun, set at 5 eV, and a metal screen placed on the sample holder. Sample charging was observed to be minimal for all the conventional polymers analyzed in this study, as indicated by their C1s line shape. This fact, combined with the reproducibility of the PDF core-level spectra, acquired at different times, strongly suggests that the PDF did not charge up during XPS analysis also.

To account for minor deviations in the transmission function and sampling depths from the assumed energy dependence for the widely separated F1s and C1s photoemission lines, poly(tetrafluoroethylene) (PTFE) samples were analyzed with the TFAA- and TFE-derivatized samples. The F/C ratio for the PTFE samples were calculated from the survey scans and normalized to the expected stoichiometric value of 2. The small hydrocarbon peak (<5 at. %) observed for PTFE provided an internal assurance that contamination of the PTFE sample was minimal. Fresh samples were always used to ensure that X-ray-induced degradation of the PTFE samples was not significant. The F/C ratios of the TFAA- and TFE-derivatized samples were then corrected by the same factor. Since the BE of the N1s photoemission line is between that of C1s and O1s, normalization of the N/C ratio for different runs was not deemed necessary.

High-resolution C1s spectra were obtained at 25-eV pass energy and 1000-μm X-ray spot size and were resolved into individual Gaussian peaks by using a least-squares fitting program. The peak positions used were in accordance with those published in the literature.[3] All peaks were initially specified with the peak position, and 1.25-eV full width half-maximum (fwhm; which is a reasonable assumption under the spectrometer conditions used). The least-squares fitting program then minimized the squared sum of differences between the composite envelope generated by the peak fitting routine and the experimentally determined envelope, by varying both the peak position and fwhm. Since the curve-fitting algorithm was not constrained with regard to either the peak position or fwhm, the final curve fit was then examined to ascertain if these values were realistic.

Static SIMS Analysis. The static SIMS experiments were performed on the SSX-100 system equipped with a static SIMS add-on (SubMonolayer Systems, Mountain View, CA). The primary ion source was a 3.5-keV, 3-nA Xe^+ beam produced from a differentially pumped Leybold-Heraeus ion gun. The ion beam current was measured by using a metallic sample stage connected directly to an electrometer. The ion beam impacted the sample at a 55° angle from the surface normal of the polymer sample. The ion beam was defocused over a 5 × 5 mm area. This resulted in current densities of 12 nA cm^{-2}. Since the total exposure time of the sample to the ion beam was <1.3 min, the total ion dose during spectral optimization and acquisition was $\sim 5 \times 10^{12}$ ions/cm^2, ensuring that static SIMS conditions were met.[36] The secondary ions were detected by a modified QMG 511 Balzers quadrupole mass spectrometer equipped with an adjustable energy filter. The takeoff angle of the detected secondary ions was 55°. A low-energy flood gun, set at 32 eV, was used to minimize sample charging. No indication of sample damage from the electrons was observed. In particular, no electron-stimulated desorption was observed (i.e., when only the electron beam was on the sample, no secondary ions were detected).

Table III. Selectivity of Derivatization Reactions

polym	functional group	derivatization reaction: TFAA XPS % F (theor)	derivatization reaction: hydrazine XPS % N (theor)
PS	C_6H_5	0	0
PBu	C=C		0
PiP	C=C	0	0
PVA	C-OH	32.6 ± 1.2 (33.3)	0
PHS	C_6H_5—OH	20.0 (20.0)	1.5
PEO	C—O—C	0	0
PVIE	C—O—C	0	0
PVMK	R—C=O	1.6	19.4 ± 1.2 (30.0)
PAA	COOH	1.1	4.4 ± 0.8
PEMA	COOR	0	0
PVAc	COOR	0	0
PET	C_6H_5—COOR		25.2 ± 0.4
PCL	R—COO—R	0	1.0

Contact Angle Measurement. Water contact angles in air were measured by the sessile drop technique on a Rame-Hart goniometer, Model 100-00-00NRL. A minimum of six measurements of contact angle with six different drops (doubly distilled deionized water) were averaged to measure the contact angle on a surface.

Scanning Electron Microscopy. The surface topography of some of the PDF were qualitatively observed by using a scanning electron microscope (SEM), Model JSM25 (JEOL Ltd., Tokyo, Japan). Samples were sputter coated with gold and then observed under the microscope, at 30° tilt, at magnifications ranging from 200× to 10000×.

Results and Discussion

Derivatization Reactions on Model Surfaces. TFAA Derivatization Reaction. While the vapor-phase TFAA derivatization reaction has been widely used to tag hydroxyl groups on surfaces,[26-28] comprehensive efforts have not been made to ascertain its specificity. XPS analysis of TFAA-derivatized model polymers revealed that both carbonyl and carboxyl groups showed low reactivity toward TFAA, evidenced by low levels of F incorporation in TFAA-derivatized PVMK and PAA (Table III). The F concentration in the TFAA-derivatized PAA represents 4 at. % of the acid groups in PAA and less than 6 at. % of the ketone groups in TFAA-derivatized PVMK within the XPS sampling depth of these polymers. On the other hand, the F concentration in TFAA-derivatized PVA (33 at. %) indicates complete reactivity of the PVA hydroxyl groups within the XPS sampling depth. Recent XPS results for TFAA derivatization of a poly(styrene/*p*-hydroxystyrene) random copolymer series indicate that phenol groups are stoichiometrically tagged only for OH concentrations greater than 4 at. %.[37] This suggests that the extent of the TFAA-derivatization reaction depends on the type (e.g., aliphatic hydroxyls versus phenols) and concentration of hydroxyl groups present. In any event, the extremely low concentrations of F detected for functional groups other than hydroxyl suggests that the vapor-phase TFAA-derivatization reaction predominantly labels hydroxyl groups when only oxygen-containing functional groups are present in the surface region and that this assay can be used to provide a semiquantitative comparison of the hydroxyl group concentrations for various oxygen-functionalized PDF.

The reaction of TFAA with PVA is illustrated by the XPS high-resolution C1s spectrum of PVA, before and after reaction. The C1s spectral envelope of PVA, shown

(33) Scofield, J. H. *J. Electron. Spectrosc. Relat. Phenom.* **1976**, *8*, 129.
(34) Application note from Surface Science Instruments 1987, Mountain View, CA.
(35) Tyler, B. J.; Castner, D. G.; Ratner, B. D. *J. Vac. Sci. Technol. A* **1989**, *7*, 1646.
(36) Briggs, D.; Hearn, M. J. *Vacuum* **1986**, *8*, 1005.
(37) Chilkoti, A.; Castner, D. G.; Ratner, B. D.; Briggs, D. *J. Vac. Sci. Technol. A* **1990**, *8*, 2274.

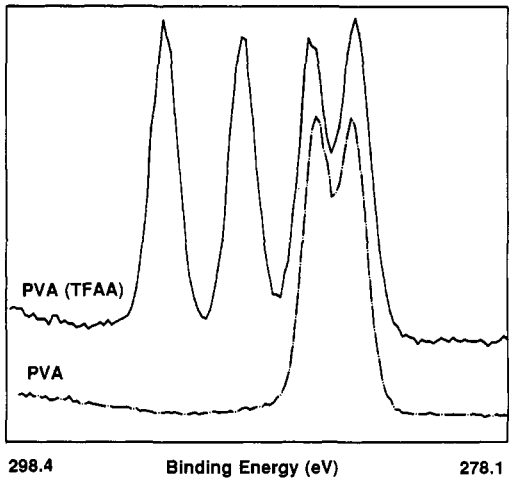

Figure 2. High-resolution C1s spectra of PVA (bottom spectrum) and TFAA-derivatized PVA (top spectrum).

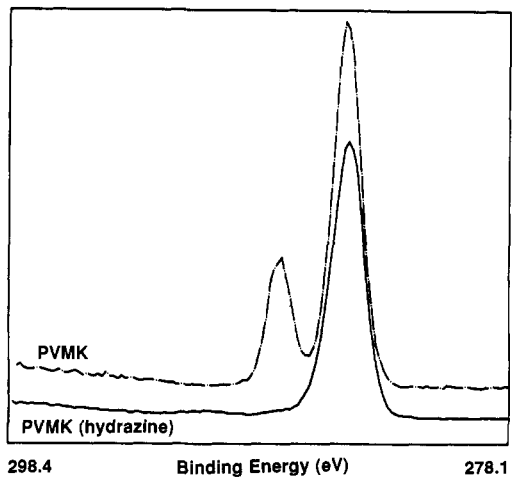

Figure 3. High-resolution C1s spectra of PVMK (top spectrum) and hydrazine-derivatized PVMK (bottom spectrum).

in Figure 2 (bottom spectrum), can be resolved into two peaks, one at 285.0 eV for CH_x species and another at 286.5 eV for COH species. The CH_x:COH peak area ratio of 1.01:1.00, determined by a least-squares fit, shows good agreement with polymer stoichiometry (1.0:1.0). The C1s spectral envelope of TFAA-derivatized PVA, shown in Figure 2 (top spectrum), required a four-peak fit. The new peaks at 289.5 and 292.6 eV can be attributed to the ester carbon and CF_3 carbon atoms, respectively. The experimentally determined CH_x:COC:CO_2:CF_3 peak area ratio of 1.2:1.0:1.0:1.0 for these peaks are close to the 1:1:1:1 ratio predicted for a stoichiometric reaction. Variable takeoff angle XPS of TFAA-derivatized PVA at 0°, 55°, and 80° showed no difference in the F/C/O ratios as a function of takeoff angle. Since the inelastic mean free path of core level photoelectrons in a polymer matrix is ~30 Å,[38] this suggests that the TFAA-derivatization reaction proceeds homogeneously over the 100-Å sampling depth.

Hydrazine Derivatization Reaction. The hydrazine derivatization reaction to tag carbonyl groups has been used to estimate the surface carbonyl concentration of CDT–poly(ethylene terephthalate) (PET).[27,28] However, no efforts were made to determine its specificity with respect to other oxygen-containing functional groups that are present in multifunctional surfaces such as CDT polymers or PDF. Also, the kinetics and reaction degree of this vapor-phase derivatization reaction were not verified.

The incorporation of N, upon reaction of PVMK with hydrazine, indicates that carbonyl groups are reactive toward hydrazine vapor. This is corroborated by the changes in the C1s spectrum of PVMK upon hydrazine derivatization. The high-resolution C1s spectrum of PVMK, shown in Figure 3 (top spectrum) can be resolved with a two-peak fit. The peak at 285.0 eV is attributed to CH_x species, while the peak at 287.8 eV is attributed to C=O species. The experimentally determined CH_x:C=O peak area ratio of 3.4:1.0 is close to the 3.0:1.0 ratio predicted for a stoichiometric polymer. Derivatization of PVMK with hydrazine vapor (1-h exposure time) resulted in the conversion of the carbonyl groups to a hydrazone, resulting in changes in the C1s spectrum (Figure 3, bottom spectrum). The intensity of the peak at 287.6 eV decreased considerably, indicating that a large fraction of the carbonyl groups have reacted with hydrazine, while the appearance of a new peak at 285.8 eV suggests the formation of a hydrazone. However, both the level of N incorporation and the presence of the residual carbonyl component in the C1s spectrum indicate that the reaction does not proceed to completion.

Calculation of the yield of this reaction from the XPS survey scans was done as follows:

$$\text{yield(N1s)} = [\%\text{N(XPS)}/\%\text{N(stoich)}]X$$

X =

[%O(stoich)/%O(XPS)] of the underivatized PVMK

A 70% yield was calculated by this method. Similarly, another value of the yield can be calculated solely on the basis of the decrease in the intensity of the O1s photoemission line, upon reaction of the ketone groups with hydrazine. Upon correction for the deviation from stoichiometry of the oxygen concentration in the surface region of underivatized PVMK, a 66% yield was calculated. Since variable takeoff angle XPS of hydrazine-derivatized PVMK indicated that N incorporation was independent of the XPS sampling depth, the yield less than 100% can be accounted for only by the reaction not proceeding to completion.

The results of the hydrazine derivatization of polymers with different oxygen-containing functionalities are shown in the fourth column of Table III. The level of N incorporation in PAA represents less than 12.0 at. % of the total carboxyl groups within the XPS sampling depth, indicating a 7-fold greater selectivity of hydrazine toward free carbonyl groups as opposed to acid carbonyl groups. Hydrazine is unreactive toward aliphatic ester groups, as observed from the lack of nitrogen incorporation upon reaction with poly(ethyl methacrylate) (PEMA), poly(vinyl acetate) (PVAc), and polycaprolactone (PCL). However, hydrazine reacts readily with aromatic esters, indicated by the nitrogen incorporation (25.2 at. %) in hydrazine-derivatized PET. The changes in the high-resolution C1s spectrum of hydrazine-derivatized PET (Figure 4, top spectrum) as compared to underivatized PET (Figure 4, bottom spectrum), notably the appearance of an amide carbon peak at 288.2 eV, corroborate this finding.

The stability of hydrazones to X-rays and electron flood was ascertained by analyzing a hydrazine-derivatized PVMK sample with XPS for times up to 5.5 h. Under the analysis conditions used (X-ray flux = 3.7×10^7 W/m^2, anode voltage = 10 kV, anode current = 20 mA, 5-eV electron flood), sequential XPS survey scans revealed no significant changes in the N/C/O atomic ratios with exposure time.

(38) Seah, M. P.; Dench, W. A. *Surf. Interface Anal.* **1979**, *1*, 2.

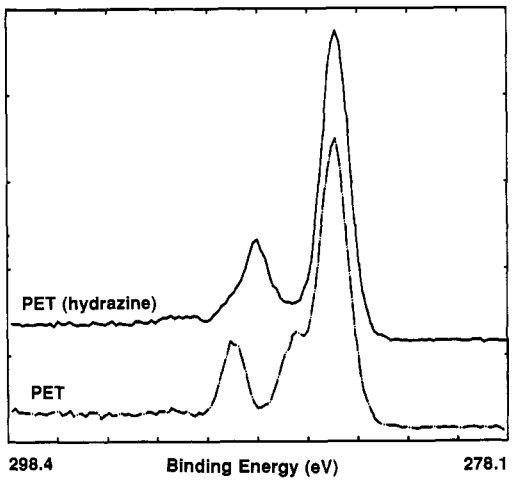

Figure 4. High-resolution C1s spectra of PET (bottom spectrum) and hydrazine-derivatized PET (top spectrum).

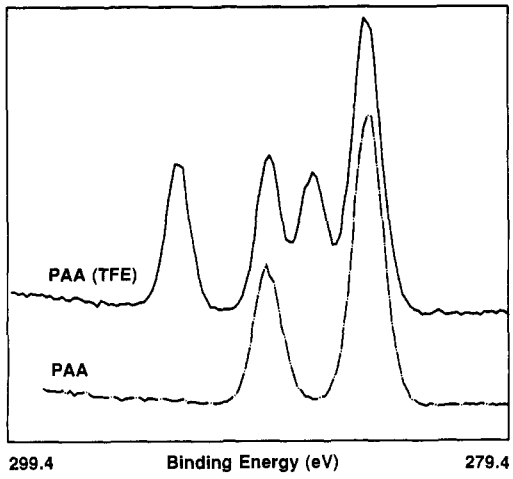

Figure 5. High-resolution C1s spectra of PAA (bottom spectrum) and TFE-derivatized PAA (top spectrum).

TFE-Derivatization Reaction. The liquid-phase reaction of carboxyl groups with TFE and dicyclohexylcarbodiimide (DCC) has been reported in the literature.[12] Since DCC is a solid at room temperature, attempts to use this reaction for a vapor-phase assay of carboxyl groups required elevated temperatures (60 °C) to attain ~60% yield.[39] These reaction conditions could result in substantial reorganization of the polymer within the XPS sampling depth, which is clearly undesirable.[40,41] Additionally, the low volatility of DCC results in adsorption of DCC or its reaction product on the surface, introducing artifacts in the quantitation of carboxyl groups.[39] The higher volatility of Di-tBuC obviates the need to use elevated temperatures and minimizes nonspecific adsorption of Di-tBuC.

The reaction of PAA with TFE and Di-tBuC results in the incorporation of fluorine, as detected by XPS. The atomic percents oxygen (20.8 ± 1.7) and fluorine (26 ± 4.8) indicate that the reaction is near stoichiometric, with a yield of 0.87 ± 0.15. The deviation in the XPS C/O/F ratio from that predicted for complete reaction for a stoichiometric polymer is due to incomplete reaction within the XPS sampling depth for some of the PAA samples,

(39) Nakayama, Y.; Takahagi, T.; Soeda, F.; Hatada, K.; Nagaoka, S.; Ishitani, A. *J. Polym. Sci.* **1988**, *A26*, 559.
(40) Everhart, D. S.; Reilley, C. N. *Surf. Interface Anal.* **1981**, *3*, 126.
(41) Everhart, D. S.; Reilley, C. N. *Surf. Interface Anal.* **1981**, *3*, 258.

Table IV. Summary of Variable Takeoff Angle XPS Results for TFE-Derivatized PAA

	takeoff angle, deg		
	80	55	0
sampling depth, Å	17	55	100
at. % oxygen	17.8	20.8	21.5
at. % fluorine	31.2	29.1	24.9
% C–O	19.4	17.0	16.3
% CF_3	20.3	16.4	12.7

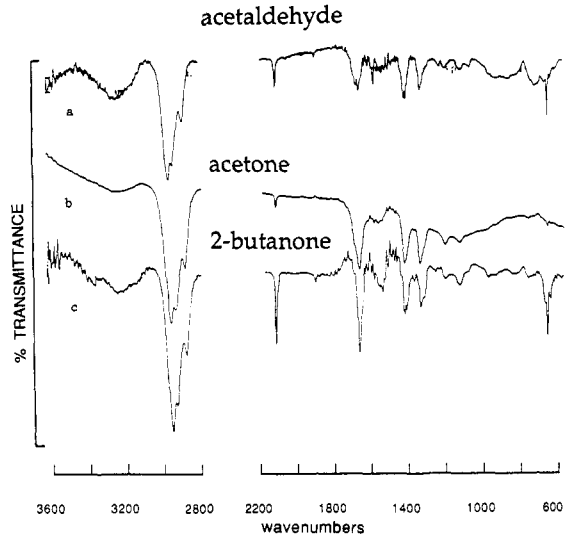

Figure 6. Transmission-FTIR spectra of plasma depositions on KBr powder, acetaldehyde (top), acetone (middle), and 2-butanone (bottom).

which would result in a higher than expected O/F ratio. Changes in the high-resolution XPS C1s spectral envelope of PAA upon derivatization with TFE corroborate the survey scan results.

The XPS high-resolution C1s spectral envelope of PAA is shown in Figure 5 (bottom spectrum). Upon derivatization with TFE, peaks at 287.2 and 292.6 eV appear, which can be attributed to COC and CF_3 species, respectively (Figure 5, top spectrum). Both the presence of this peak and the COC:CO_2:CF_3 peak area ratio of 1.1:1.1:1.0 indicate that nearly all the PAA acid groups are labeled within the XPS sampling depth (i.e., ~50 Å) for this sample. This was confirmed by the 30 at. % F incorporation measured in the survey scan spectra for this sample.

The results of variable takeoff angle XPS for this sample are shown in Table IV. The decrease in the atomic percent fluorine and in the percentage areas of the CF_3 and CO peaks (least-squares fit of the high-resolution XPS C1s spectrum) as a function of sampling depth indicates that the reaction is not homogeneous over the entire 100-Å sampling depth. Rather, below the top 50 Å, some fraction of the PAA acid groups are not labeled. The selectivity of this reaction should be similar to the TFE/DCC derivatization reaction, which was found to be selective toward carboxyl groups as compared to hydroxyl and ester groups.[40] The selectivity of this reaction has been ascertained by reaction with a variety of polymers containing different oxygen functional groups and has been found to be excellent with respect to carboxyl groups.[32] These results suggest that this derivatization procedure may be used for the semiquantitative estimation of carboxyl groups.

Prolonged exposure of TFE-derivatized PAA to X-rays (200 W) and electron flood (5 eV) for up to 2.3 h did not result in significant changes either in the XPS C/O/F

ratios or in the shape of the high-resolution C1s spectral envelope. Thus, sample degradation was minimal under the analysis conditions used.

Acetaldehyde, Acetone, and 2-Butanone Plasma Depositions. FTIR Results. The transmission-FTIR spectra of KBr powder exposed to plasmas of the three precursors are shown in Figure 6. The primary features of all three spectra are identical despite the differences in precursor type. The principal hydrocarbon moieties identified by FTIR were the CH_3 and the CH_2 groups. The CH_3 group was identified by assignment of peaks at 2960.0 and 2872.4 cm^{-1} to the C–H stretch in the asymmetric and symmetric mode of the CH_3 group, respectively, while the CH_2 group was identified by assignment of the major peak at 2930.8 cm^{-1} to the asymmetric vibration of the H atom.[42] Corroboration of these assignments was provided by a peak at 1461.6 cm^{-1}, which was assigned to the asymmetric C–H deformation of the CH_3 group and/or C–H bending of the CH_2 group, and peaks at 1380 and 1245 cm^{-1}, which were assigned to the symmetric C–H deformation of the CH_3 group and C–H twist of the CH_2 group, respectively.

The principal oxygen-containing functional groups identified by transmission FTIR analysis were the ketone carbonyl at 1710 cm^{-1} and a broad, diffuse band at 3200–3500 cm^{-1}, which was assigned to an –OH stretch.[42] The contribution of adsorbed water to the observed –OH stretch was explored by drying the KBr pellet in a vacuum desiccator at 60 °C for 24 and 48 h, respectively. The intensity of the band between 3200 and 3600 cm^{-1} decreased considerably with time, which suggests that adsorption of water contributes to the observed intensity of this band.

XPS Results. XPS survey scans of all three PDF were similar and revealed incorporation of oxygen, presumably from the precursor. Nitrogen was not detected in any of the PDF, indicating that the effect of residual air in the plasma was minimal. Figure 7a shows the atomic percent O incorporated in these PDF, as determined by XPS. Each bar represents the average of four different reaction runs for each precursor. The error bars represent 1 standard deviation for each data set. The results indicate that the atomic percent oxygen incorporated is not a function of the C/O ratio of the precursor, under the experimental conditions used.

The high-resolution C1s spectra of all three PDF were similar in shape and showed distinct features compared to untreated PS. Least-squares peak fitting of the high-resolution C1s spectra of the three types of PDF was carried out. The fit was specified by peaks representative of CH_x species (285.0 eV), COR species (alcohols, ethers, epoxides, and hydroperoxides, 286.5–286.6 eV), and RC=O species (aldehydes and ketones, 287.7–288.0 eV). Peak areas for a fourth acid/ester group were close to zero. The results of the least-squares fit of the C1s spectral envelope suggest that C–O species (ether, hydroxyl, peroxides and epoxides) and carbonyl type functionalities (ketones and aldehydes) are present in these PDF and that the concentration of acid/ester species is negligible.

The appearance of a F peak in the XPS survey scan spectra of the TFAA-derivatized PDF indicates the presence of hydroxyl groups. Figure 7b shows the atomic percent F incorporation, measured from XPS survey scans, for the three TFAA-derivatized PDF. The F concentrations are in the same range for all three PDF, suggesting that the C/O ratio of the precursor does not influence the extent of hydroxylation of these films. N is observed in

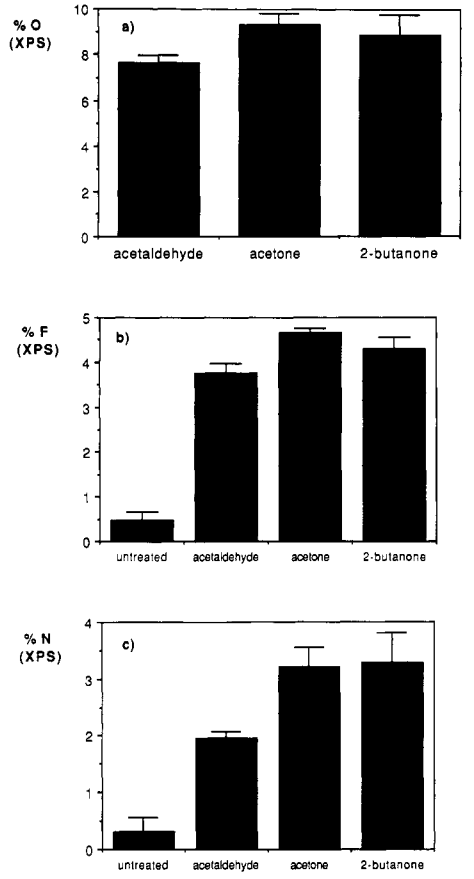

Figure 7. Acetaldehyde, acetone, and 2-butanone PDF: (a) XPS % O, (b) XPS % F (TFAA-derivatized), (c) XPS % N (hydrazine derivatized).

the XPS survey scan spectra of all three PDF after hydrazine derivatization, indicating the conversion of surface carbonyl groups to hydrazones. The N incorporation for the hydrazine-derivatized PDF was calculated from the survey scans and is reported in Figure 7c. Variable takeoff angle XPS of the acetone PDF sequentially derivatized with TFAA and hydrazine showed no significant differences in the atomic percent F and N as a function of sampling depth (10–100 Å), indicating that these PDF are homogeneous (within the detection limits of XPS) over the range of sampling depth.

Experiments on the kinetics of the hydrazine derivatization reaction indicated that under the reaction time used for these samples (i.e., 15 min) ~60% of the carbonyl groups are tagged. Correcting the values obtained for the XPS measured surface nitrogen incorporation would then result in a maximum nitrogen incorporation of ~6 at. %. The low level of nitrogen incorporation for all three PDF is indicative of extensive fragmentation of the precursor molecules in the plasma, leading to low retention of the carbonyl-containing fragments in the resulting PDF. The data also suggest that of the three types of depositions, the acetaldehyde plasma is the least successful in incorporating carbonyl groups, while the size of the error bars for the other two depositions suggests similar levels of N incorporation. Since these groups are incorporated from fragments of the parent molecule, we postulate that fragments from the parent molecule containing the carbonyl group are more likely to be incorporated in the growing PDF if they contain one or more hydrocarbon moieties; in the case of acetaldehyde, the fraction of such species would be reduced in view of the structure of the parent molecule. Conversely, the creation of such fragments in the acetone

(42) Conley, R. T. *Infrared Spectroscopy*; Allyn and Bacon: Boston, 1972.

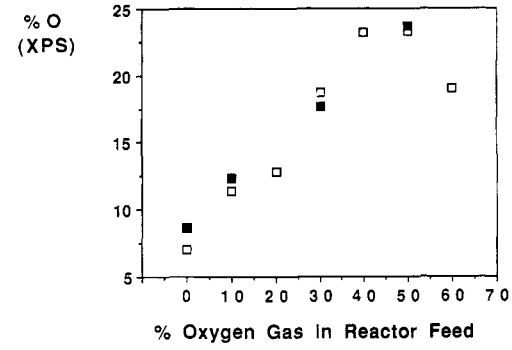

Figure 8. XPS-measured percent O for the acetone–O_2 PDF versus percent flowrate of O_2 gas in reactor feed: filled squares, set I; open squares, set II.

and 2-butanone plasma is more probable.

Evans et al. have shown that under conditions of low power dissipated per molecule, the plasma polymerization of vinylic monomers such as styrene is similar to conventional free-radical-initiated polymerization.[43] For a styrene plasma initiated at low power, direct mass spectrometric evidence that the parent molecule and parent radical cation are the predominant species in the plasma suggests that fragmentation of the precursor is minimal.[44]

In the case of conventionally polymerizable precursors such as vinylic monomers, a low degree of precursor fragmentation can be rationalized on the basis of the preferred locus of polymerization at the double bond, in view of the low bond dissociation energies. At low power dissipated per molecule, the distribution of species will thus favor parent species (i.e., radical ions and neutrals).[45] Additionally, we may presume that ion energies in the sheath are low enough not to cause ion-impact-induced dissociation of the surface species. Hence, even though the power per molecule values for the carbonyl plasmas are in the same range as in the styrene polymarization of Ferreiro et al.,[44] since there is no preferred locus for polymerization, i.e., the CH, CC, and C=O bond energies are very similar,[45] precursor fragmentation is relatively indiscriminate. Additionally volatile species such as CO and H_2O are formed,[45] which may not readily incorporate in the polymer. Such factors may be responsible for the low degree of precursor structure retention and consequently low oxygen concentration in these PDF.

Acetone–O_2 Plasma Depositions. Adding O_2 to the acetone feed did not lead to a significant increase in pressure upon generating the plasma, as compared to the pressure increase observed for the pure acetone plasma. This suggests that fragmentation of the gas-phase species dominates over deposition on the substrate (and walls of the reactor) but that this effect is not exacerbated by the addition of O_2 for the reaction conditions utilized. The effect of introducing oxygen gas in the feed stream on the oxygen incorporation in the acetone–O_2 PDF, as determined from XPS survey scans, is shown in Figure 8. The oxygen incorporation in these PDF reaches a maximum between 40 and 50% O_2 in the feed stream. Also, the agreement in the XPS results between the two data sets is excellent, demonstrating that these PDF can be reproduced. The graded oxygen incorporation in the acetone–O_2 PDF is corroborated by the high-resolution C1s spectra of these films, shown in Figure 9. The spectra illustrate

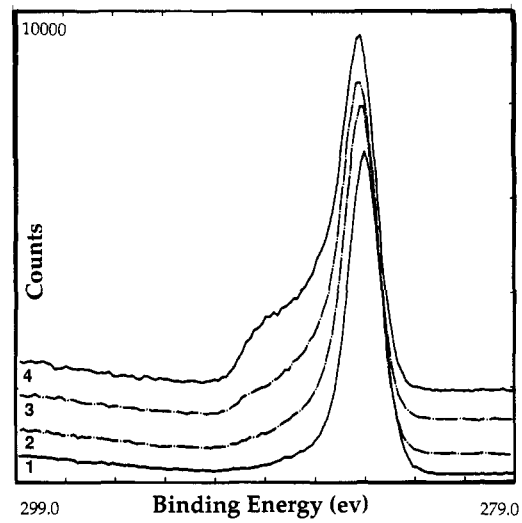

Figure 9. High-resolution C1s spectra of acetone–O_2 PDF: (1) acetone, (2) 10% O_2 in feed, (3) 30% O_2 in feed, (4) 50% O_2 in feed.

the increase in the fraction of oxygenated species relative to CH_x species, with increasing O_2 content in the feed.

Similar results have been reported by Prohaska et al. for plasma deposition from mixtures of ethylene and O_2.[46] Specifically, they observed an increase in the surface oxygen incorporation with increasing fraction of O_2 in the ethylene feed. However, saturation in surface oxygen incorporation for the ethylene/O_2 PDF was observed to occur at 10% O_2 fractional feed rate (with respect to ethylene feed rate) as compared to 66% O_2 feed rate (with respect to acetone feed rate) for the acetone–O_2 PDF. The C1s spectra of the ethylene–O_2 PDF indicated the presence of a variety of oxygen-functionalized species, similar to the acetone–O_2 PDF. However, the C1s spectra for the surface oxygen-rich ethylene–O_2 PDF differ from the oxygen-rich acetone-O_2 PDF notably in one respect, namely, the presence of carbonate species. The presence of carbonate species for the ethylene–O_2 PDF, absent in the acetone–O_2 PDF, argues that the ethylene–O_2 PDF are more dehydrogenated than the acetone–O_2 PDF. These differences in PDF surface chemistry suggest that the mechanism of oxygen incorporation in the PDF for the two precursor mixtures may be different.

The composition as a function of depth of the acetone–O_2 PDF was also investigated. The 50% oxygen (in feed) PDF from set I and the 40% oxygen (in feed) PDF from set II were examined by XPS at 0° and 80° takeoff angles. The XPS measured percent oxygen showed little variation with changes in the XPS sampling depth, indicating that these modified surfaces are homogeneous and at least 100 Å thick. Additionally, variable takeoff angle XPS of a TFAA- and hydrazine-derivatized acetone–O_2 PDF sample (60% oxygen in feed, set II) showed no significant variation in the fluorine and nitrogen incorporation with change in XPS sampling depth, suggesting the absence of concentration gradients for the hydroxyl and carbonyl groups in the top 100 Å.

With increasing enrichment of oxygen species in the acetone–O_2 PDF, the advancing water contact angle in air decreases, indicating the increased hydrophilic nature of these surfaces (Figure 10). XPS data on the stability of the acetone–O_2 PDF upon storage in air for over ~6 months are shown in Table V. The acetone–O_2 PDF

(43) Evans, J. F.; Prohaska, G. W. *Thin Solid Films* **1984**, *118*, 171.
(44) Ferreiro, L. M.; Ernie, D. W.; Evans, J. F. *J. Vac. Sci. Technol. A* **1987**, *5*, 430.
(45) Yasuda, H. *Plasma Polymerization*; Academic Press: New York, 1985.
(46) Prohaska, G. W.; Nickson, C. G. *J. Polym. Sci. A: Polym. Chem.* **1989**, *27*, 2633.

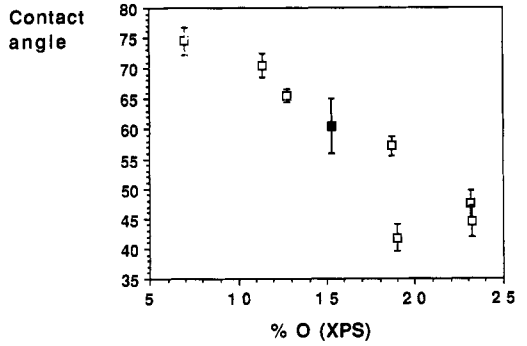

Figure 10. Advancing water contact angle in air: open squares, set II, acetone–O_2 PDF; filled squares, Falcon TCPS surface.

Table V. Stability of Acetone–O_2 PDF

	XPS O/C ratios[a]		
% O_2 in feed	A	B	C
0	0.08	0.10	0.11
10	0.13	0.15	0.13
20	0.15		0.16
30	0.23	0.24	
40	0.30	0.32	0.30
50	0.30	0.27	0.22 ± 0.03
60	0.24	0.22	0.18

[a] A = XPS analysis at time of deposition. B = XPS analysis 6 months later. C = XPS analysis of samples B soaked in DI water for ~12 h.

retain their original levels of oxygen incorporation. Also, exposing these PDF to deionized water under ambient conditions for ~12 h had little effect on their oxygen content. This suggests that the oxygen species in the surface region are covalently incorporated in the plasma polymer. On the basis of the above data, blending in O_2 gas in the acetone feed is a viable method for creating oxygen-rich PDF that are hydrophilic in nature and are stable.

A possible effect of using gas mixtures containing a plasma polymerizable precursor and an etchant, particularly at higher O_2 plasma feed concentrations, is the introduction of surface roughness. The introduction of surface roughness as a function of treatment time has been observed for PTFE etched with an O_2 plasma.[47] To ascertain if the surface topography of these PDF is altered by the introduction of O_2 gas in the feed stream, the surfaces of the acetone–O_2 PDF were observed by SEM, up to 10000× magnification. No surface topography was seen on either the acetone or acetone–O_2 PDF.

Comparison of the XPS analysis of the acetone–O_2 PDF with a commercially available TCPS surface (Falcon) is instructive. The level of oxygen incorporation in the TCPS surface, ~15 at. % as determined by XPS, lies within the range achievable with the acetone–O_2 PDF. In comparison with the acetone–O_2 PDF, the high-resolution C1s spectrum of the Falcon TCPS surface, shown in Figure 11, is suggestive of differences in surface structure. A four-peak fit, similar to that employed for the acetone–O_2 PDF was attempted for the TCPS surface. No constraints on the peak fit were employed except to specify peaks representative of hydrocarbon species (285.0 eV), ether/hydroxyl/peroxide/epoxide species (286.5 eV), carbonyl type groups (287.8 eV), and acid/ester groups (289.0 eV). The least-squares fit showed that to keep the fwhm of these peaks within the same range as for the acetone–O_2 PDF, a peak at 291.7 eV had to be introduced. Least-squares

(47) Morra, M.; Occhiello, E.; Garbassi, F. *Langmuir* **1989**, *5*, 1989.

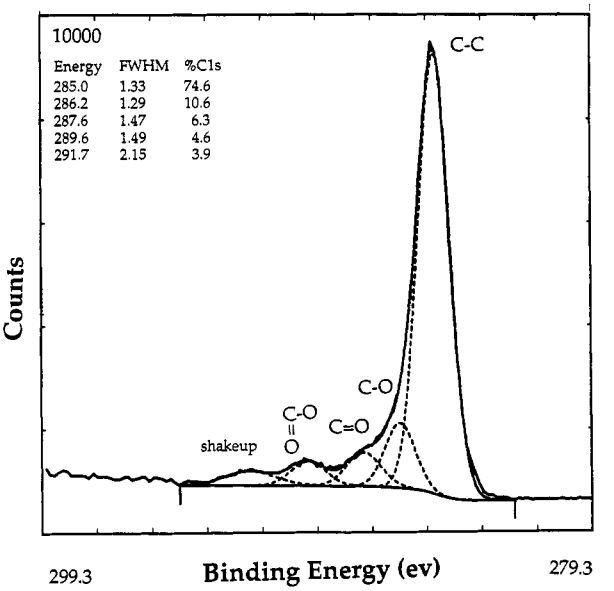

Figure 11. Least-squares peak fit of high-resolution C1s spectrum of Falcon TCPS surface.

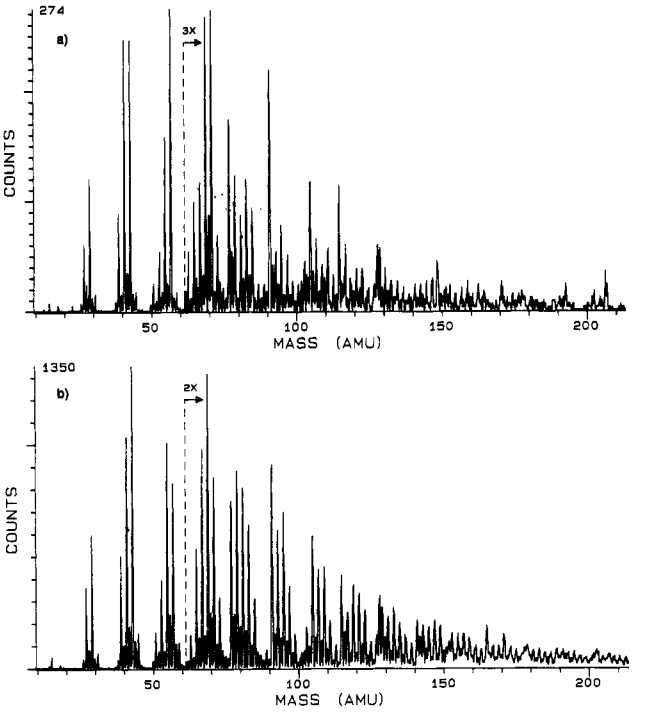

Figure 12. Positive static SIMS spectra: (a) Falcon TCPS surface, (b) acetone PDF on PS.

peak fitting of the C1s spectral envelope with five peaks then led to similar and plausible fwhm for all peaks, except the peak centered at 291.7 eV. The fwhm of the peak at 291.7 eV was uncharacteristically broad (2.1 eV). The position of this peak, combined with its large fwhm, suggests that it can be attributed to a π–π^* shakeup satellite, commonly observed in unsaturated polymers.[3]

Evidence for the differences in the surface chemistry of the Falcon TCPS surface and the acetone PDF, including the partial retention of the aromatic nature of the PS substrate in the Falcon TCPS surface, is found by comparing the positive static SIMS spectrum of an acetone PDF with that of the Falcon TCPS surface (Figure 12). The fingerprint spectra of the two surfaces are different. First, in contrast to the acetone PDF, where the base peak is at 43 D peak, the base peak for the Falcon TCPS surface

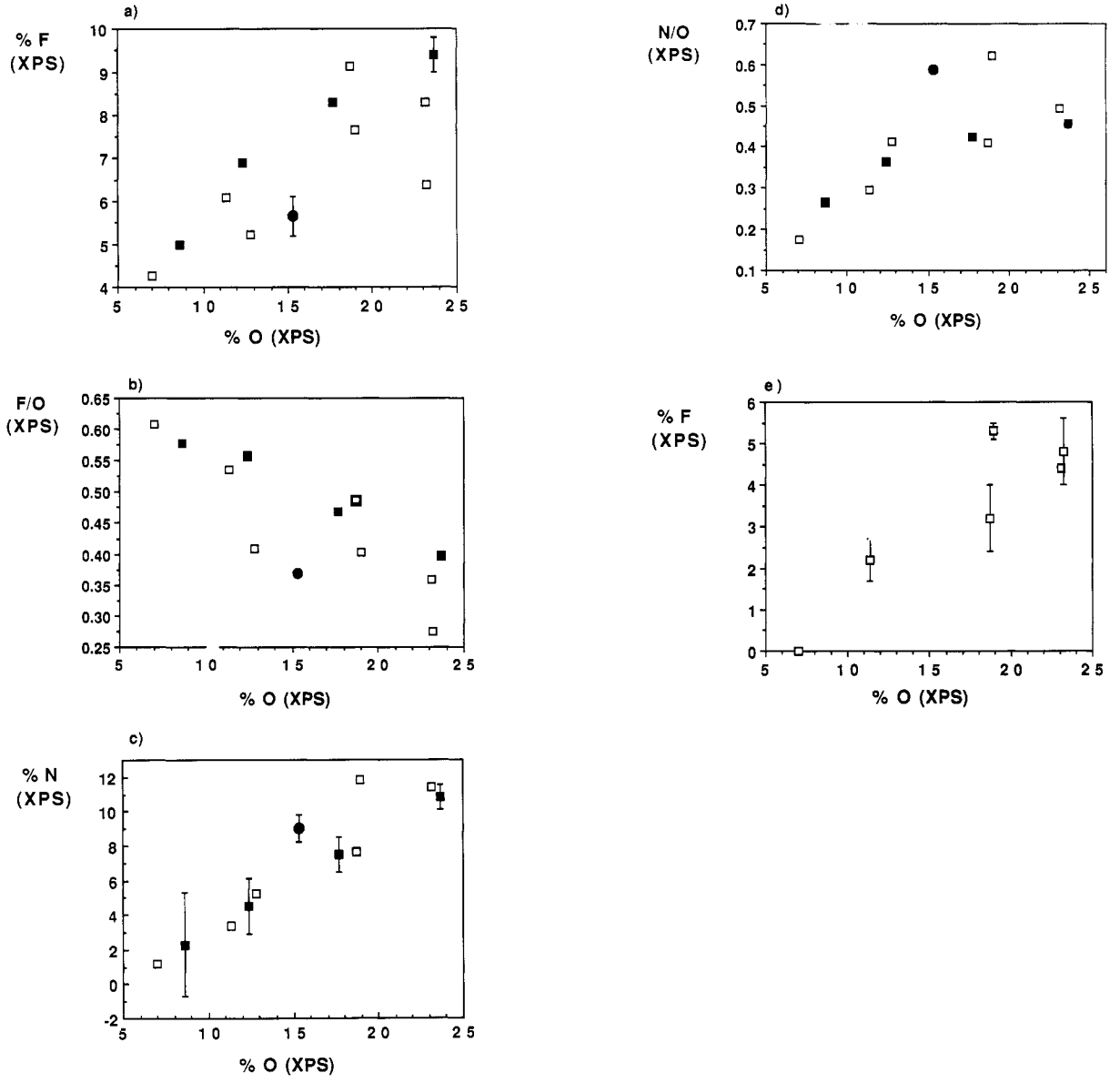

Figure 13. Acetone–O_2 PDF series derivatization results: (a) XPS measured, atomic percent F (TFAA derivatized) versus atomic percent O (underivatized); (b) ratio of (XPS measured) atomic percent F (TFAA derivatized) to atomic percent O (underivatized) versus atomic percent O; (c) (XPS measured) atomic percent N (hydrazine derivatized) versus atomic percent O (underivatized); (d) ratio of (XPS measured) atomic percent N (hydrazine derivatized) to atomic percent O (underivatized) versus atomic percent O (closed squares, set I acetone–O_2 PDF), (open squares, set II, acetone–O_2 PDF), (closed circle, Falcon TCPS surface); (e) XPS measured atomic percent F (TFE derivatized) versus atomic percent O (underivatized).

is at 57 D. Thus, while a large fraction of the oxygen species present in the acetone PDF are manifest in the CH_3CO^+ ion, such species from the Falcon TCPS are probably accounted for by the $C_3H_5O^+$ ion. Second, the intensity of the 77, 91, 105, and 115 D ions (indicative of aromaticity)[48,49] relative to neighboring peaks is greater for the Falcon TCPS surface as compared to the acetone PDF. The negative ion spectra (not shown) for both the acetone PDF and the Falcon TCPS surface are simple. The primary peaks are due to C_n^-–C_nH^- (n = 1–4) (characteristic of aliphatic and aromatic HC polymers),[48-50] O^-, and OH^-. These observations suggest that the underlying aromatic structure of the PS substrate is not completely destroyed during surface modification, corroborating the XPS results.

The results of the XPS analysis of the TFAA-derivatized acetone–O_2 PDF are shown in Figure 13a. Though the scatter in the data is large, the data suggest that there is a general increase in the hydroxyl concentration with increasing oxygen incorporation. However, the observed decrease in the XPS F (TFAA derivatized) to O (underivatized) ratio (Figure 13b) indicates that the concentration of hydroxyl groups relative to total oxygen incorporation decreases with increasing concentration of oxygen-containing species. The Falcon TCPS surface falls within the general trend observed for the acetone–O_2 PDF. The appearance of a CF_3 peak at ~293 eV in the high-resolution C1s spectrum of the oxygen-rich acetone–O_2 PDF corroborates the appearance of F in the survey scan spectra of the acetone–O_2 PDF.

The results of the hydrazine derivatization reaction for both sets of acetone–O_2 PDF are shown in Figure 13c. A direct correlation between the surface oxygen incorporation

(48) Briggs, D.; Brown, A.; Vickerman, J. C. *Handbook of Static Secondary Ion Mass Spectrometry (SIMS)*; Wiley: Chichester, 1989.
(49) Chilkoti, A.; Castner, D. G.; Ratner, B. D. *Appl. Spectrosc.*, in press.
(50) Van Ooij, W. J.; Brinkhuis, R. H. G. *Surf. Interface Anal.* **1988**, *11*, 430.

and the absolute concentration of carbonyl groups is observed, similar to the results of the hydroxyl derivatization procedure. However, unlike the relative concentration of hydroxyl groups (relative to total oxygen incorporation), which decreased with increasing oxygen incorporation, the relative carbonyl concentration (indicated by the ratio of N (hydrazine derivatized) to O (underivatized)) increases with increasing oxygen incorporation (Figure 13d). These results suggest that the distribution of surface-oxygen species changes substantially as the ratio of acetone to O_2 gas is varied in the reactor feed. Additionally, the oxygen-rich acetone–O_2 PDF are enriched in carbonyl type functionalities. Assuming that the stoichiometry and kinetics for the reaction of hydrazine with the acetone–O_2 PDF is similar to that observed for PVMK, the maximum levels of N incorporation observed for some of the hydrazine-derivatized acetone–O_2 PDF (~12 at. %) could represent surfaces where up to ~50% of the surface oxygen species are carbonyl type functionalities.

The data presented in Figure 13c also provide information about the sensitivity of the hydrazine derivatization reaction. An inverse correlation is observed between the standard deviation in the N incorporation due to hydrazine tagging and the level of N incorporation. Below 2% N labeled in the PDF, the standard deviation exceeds 100%, indicating that at low levels of N incorporation, the quantitation of C=O groups by hydrazine derivatization is imprecise. The precision of the hydrazine derivatization procedure improves considerably above concentrations of carbonyl groups corresponding to a 4% N tag.

Least-squares peak fitting of the high-resolution C1s spectral envelope of the acetone–O_2 PDF and the TCPS surface suggested an appreciable concentration of acid/ester groups compared to the acetone PDF. Since the XPS BE shifts of acid and esters are virtually indistinguishable, the acetone–O_2 PDF and the TCPS surface were derivatized with TFE to selectively label the acid groups.

The results of the TFE derivatization for the acetone–O_2 PDF (set II) are shown in Figure 13e. The reported values of fluorine concentrations represent an upper bound to the carboxyl groups (since they have been normalized to 100% yield for PAA). The increase in the XPS measured fluorine concentration indicates increasing absolute concentration of carboxyl groups with oxygen incorporation. However, the maximum fluorine incorporated indicate that less than 10% of the oxygen incorporated is in the form of carboxyl groups.

Summary

Investigation of the surface chemistry of PDF created from acetaldehyde, acetone, and 2-butanone demonstrated that under controlled experimental conditions the effect of varying the precursor C/O ratio was minimal. The resulting films were primarily hydrocarbon and lightly functionalized with oxygen-containing functional groups. The concentration of the functional groups of interest, viz., hydroxyl and carbonyl, was low. The above observations, particularly the low PDF carbonyl concentrations, suggest extensive fragmentation of the precursor in the gas phase and the substrate sheath.

It was demonstrated that oxygen-rich PDF that were stable both in air and in water could be reproducibly created from mixtures of acetone and oxygen. The surface enrichment of oxygen in these films was related to the addition of O_2 gas to the acetone feed. The results of the TFAA and hydrazine derivatization XPS results indicate that the distribution of hydroxyl and carbonyl functional groups varies across the range of oxygen incorporation in these PDF. This is probably related to changes in the plasma environment with the addition of O_2 gas in the reactor feed. However, in the absence of plasma diagnostic information, no hypothesis regarding such changes is advanced. Additionally, both XPS and static SIMS suggest that the surface chemistry of the TCPS surface differs significantly from both the pure acetone PDF and the acetone–O_2 PDF. The implications of the differences between the surface chemistry of the acetone–O_2 PDF and the commercial TCPS surface on bovine aortic endothelial cell growth will be discussed in a forthcoming publication.

Acknowledgment. Generous support received from NIH Grant RR01296 made these studies possible. We thank Drs. Peter Edelman and Thomas Lenk for help with the FTIR spectrometer, Deborah Leach-Scampavia for generating static SIMS spectra, and Winston Ciridon for assistance with the SEM. We also thank C. S. Lyons and G. A. Korba of 3M Corp. for providing us the protocol for the TFE derivatization reaction.

Note Added in Proof. Recent results from our laboratory, as yet unpublished, indicate that epoxides display a reactivity toward TFAA vapor similar to that of hydroxyls. Since we do not have conclusive evidence to rule out the presence of epoxides in these PDF, the XPS-measured atomic percent F for the TFAA-derivatized PDF must be interpreted as a measure of the relative concentration of hydroxyl and epoxide groups.

Registry No. PS, 9003-53-6; TFE, 75-89-8; PBu, 9003-17-2; PiP, 9003-31-0; PVA, 9002-89-5; PHS, 24979-70-2; PEO, 25322-68-3; PVIE, 9003-44-5; PVMK, 25038-87-3; PAA, 9003-01-4; PEMA, 9003-42-3; PVAc, 9003-20-7; PCL, 24980-41-4; TFAA, 407-25-0; O_2, 7782-44-7; di-*t*-BuC, 691-24-7; acetaldehyde (homopolymer), 9002-91-9; acetone (homopolymer), 27073-87-6; 2-butanone (homopolymer), 29115-77-3; hydrazine, 302-01-2.